Electronic Supplementary Information (ESI)

Enhanced sorption in an indium-acetylenedicarboxylate metal-organic framework with unexpected chains of *cis*-μ-OH-connected {InO_6} octahedra

Dennis Woschko, Süheyla Yilmaz, Christian Jansen, Alex Spieß, Robert Oestreich, Tobie Matemb Ma Ntep, Christoph Janiak*

Institut für Anorganische Chemie und Strukturchemie, Heinrich-Heine-Universität Düsseldorf, Universitätsstraße 1, 40225 Düsseldorf, Germany.
* *Corresponding author*: C. Janiak Tel.: +49 211 81 12286; fax: +49 211 81 12287.

Emails: dennis.woschko@hhu.de, sueheylaylmz@gmail.com, christian.jansen@hhu.de, alex.spiess@hhu.de, robert.oestreich@hhu.de, tobie.matemb.ma.ntep@hhu.de, janiak@uni-duesseldorf.de

Keywords: Metal-organic frameworks, indium, linear linker, *cis*-μ-OH-connected polyhedra, chiral space group, gas adsorption, hydrogen, heat of adsorption, vapor adsorption, volatile organic compounds (VOCs), IAST selectivity.

The adsorption data is also supplied as separate files in AIF format as part of the ESI.

Content

Section S1: Characterization of HHUD-4 and In-fum

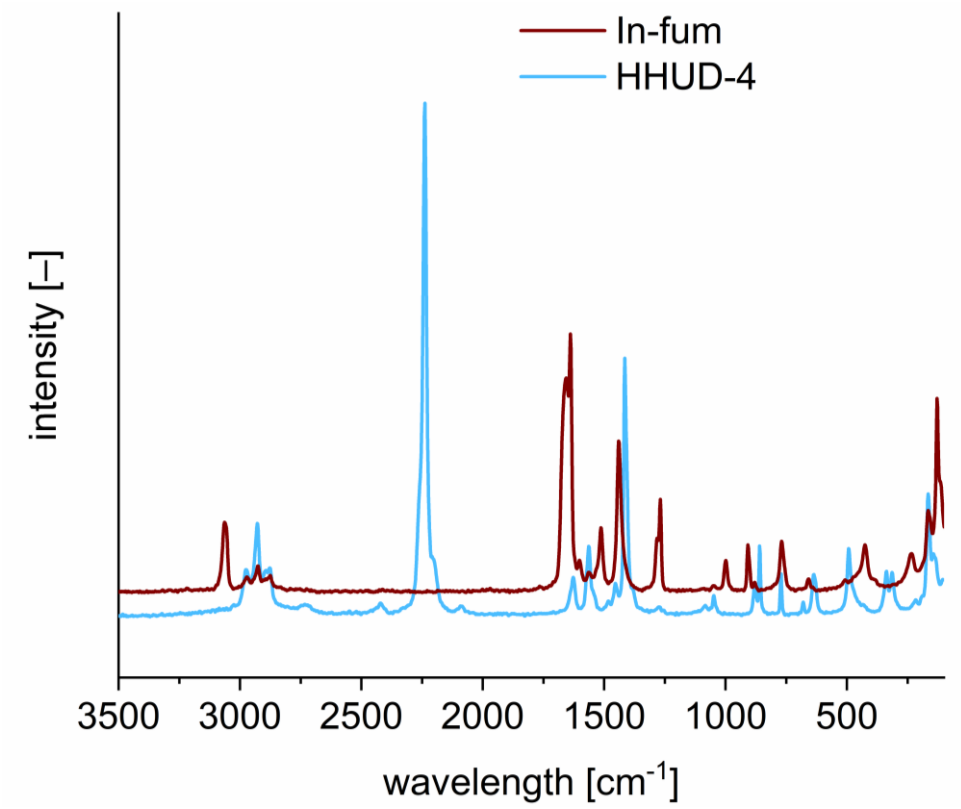

Figure S1. Raman spectra of HHUD-4 and In-fum in the range from 3500 to 100 cm^{-1}.

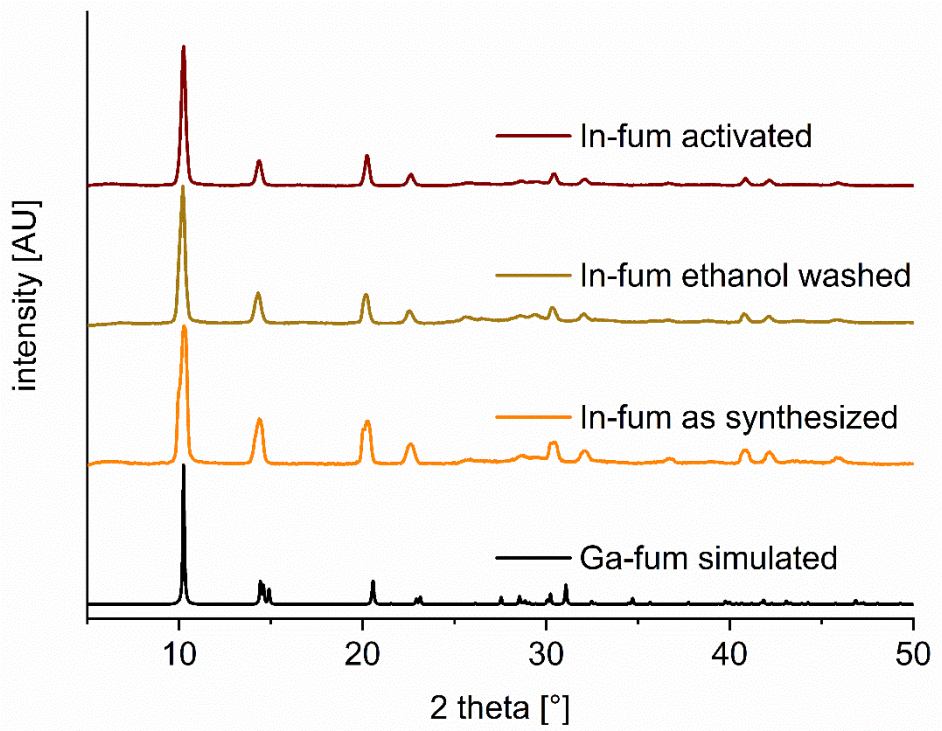

Figure S2. Comparison of the experimental powder X-ray diffractograms, PXRDs of In-fum (no X-ray structure available) after sequential activation steps with the simulated pattern of Ga-fum from the deposited cif file with CCDC no. 1838533.[1]

a)

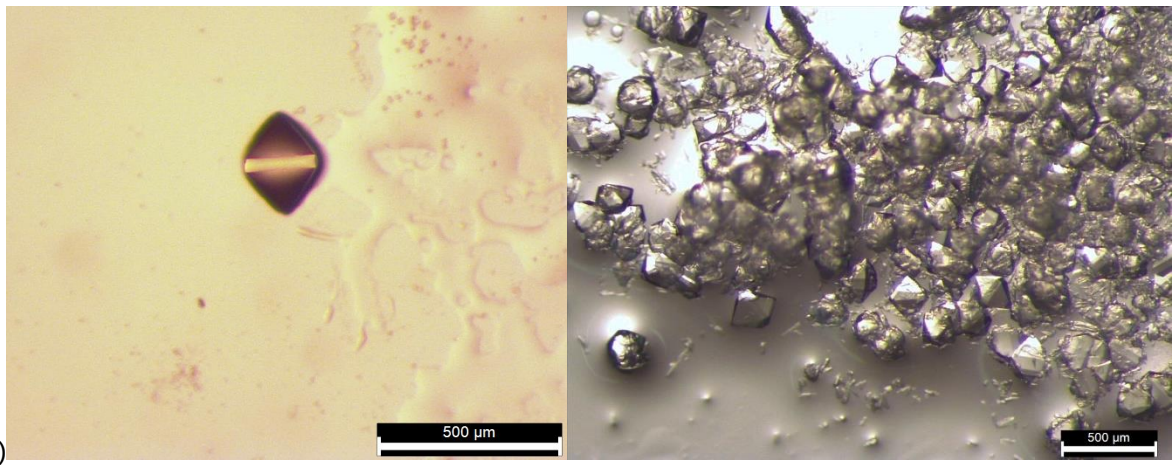

b)

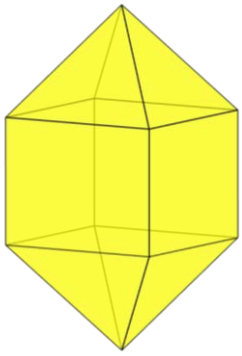

Figure S3. a) Optical microscopy images of single crystals of HHUD-4 directly obtained from synthesis. b) The predicted crystal habit of a bicapped square prism from the Bravais, Friedel, Donnay and Harker (BFDH) algorithm embedded in MERCURY.[2]

a)

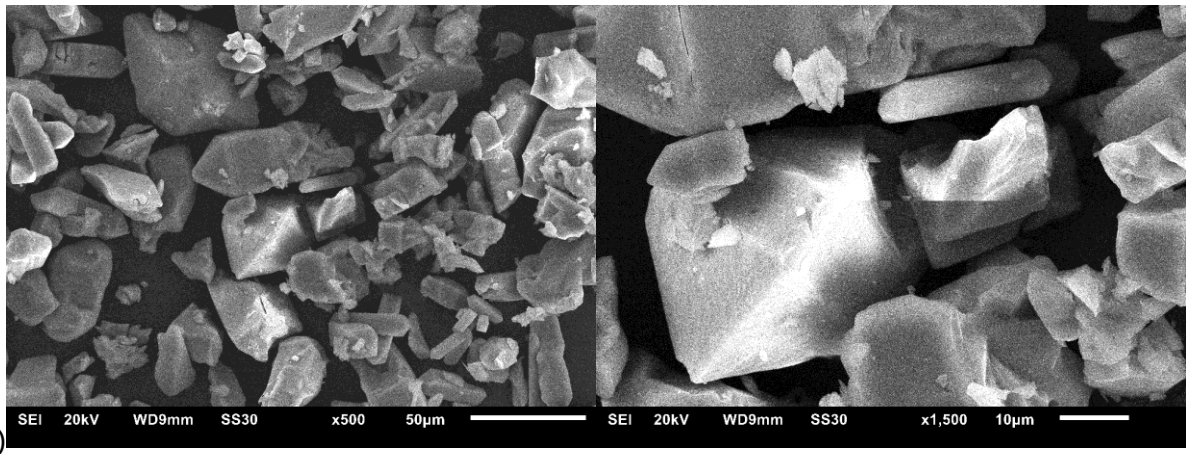

b)

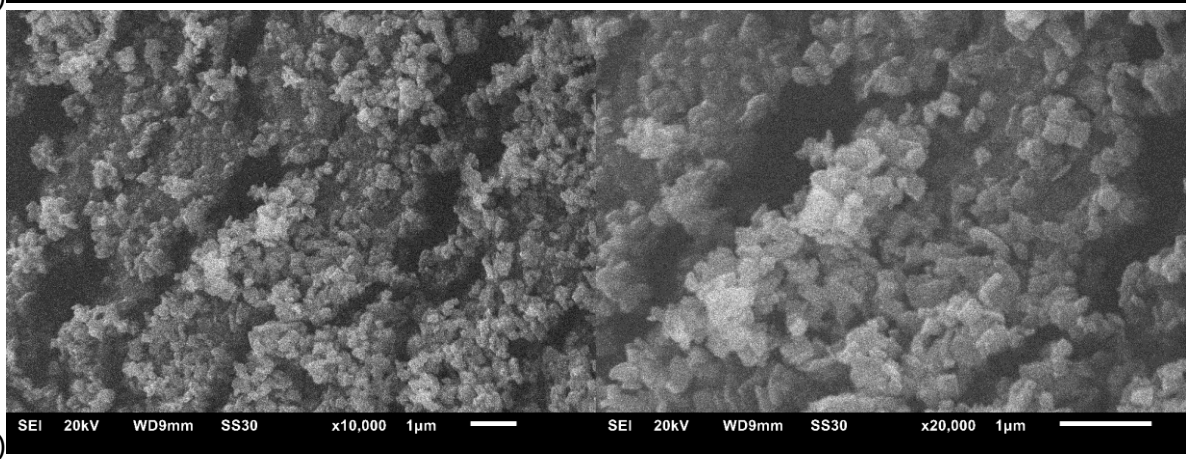

Figure S4. SEM images of a) HHUD-4 and b) In-fum.

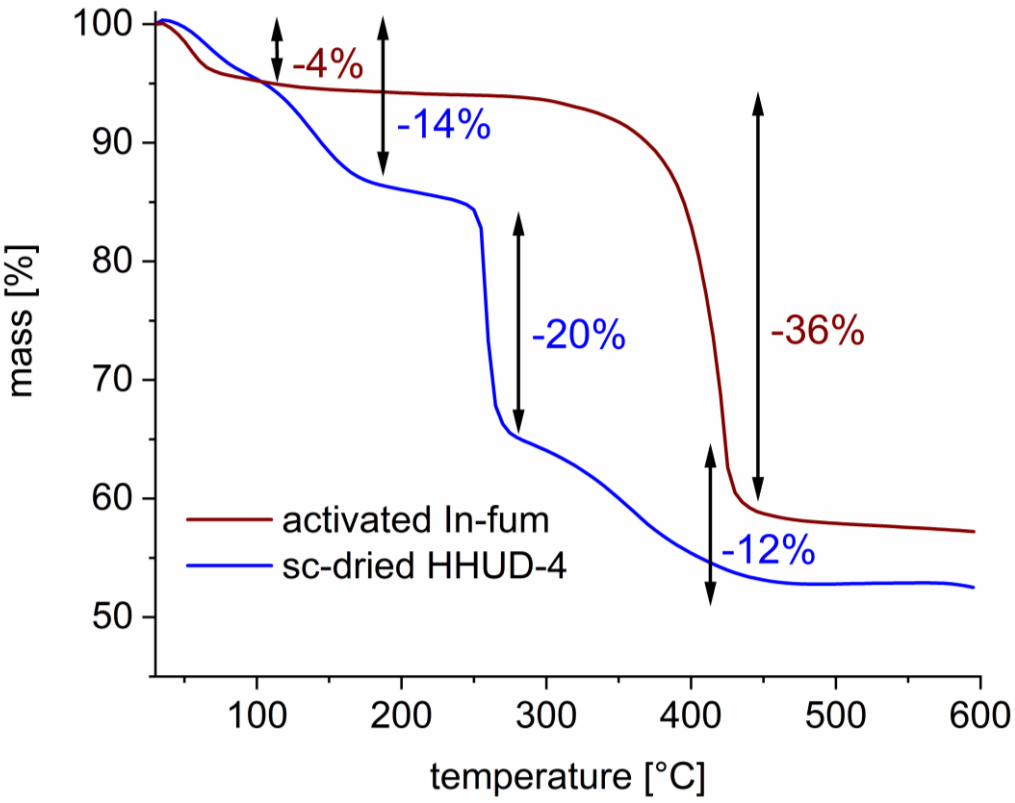

Figure S5. Thermogravimetric analysis of HHUD-4 and In-fum after supercritical (sc) drying or activation under vacuum at 100 °C for 3 h. TGA was carried out under nitrogen with a heating rate of 5 K min^{-1}.

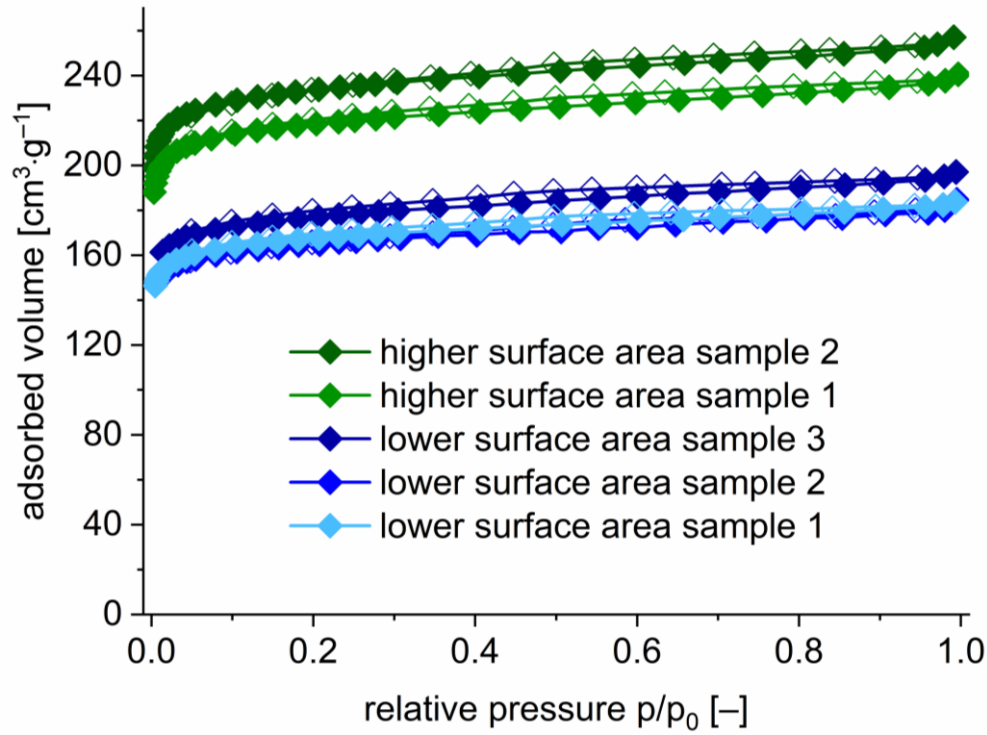

Figure S6. Volumetric nitrogen sorption isotherms of different samples of HHUD-4 (filled symbols for adsorption, empty symbols for desorption).

Table S1. BET surface areas and pore volumes of different HHUD-4 samples synthesized and washed under the same conditions.

sample	BET surface area [m^2 g^{-1}]	pore volume at p/p_0 = 0.95 [cm^3 g^{-1}]
high surface sample 2	938	0.391
high surface sample 1	878	0.366
low surface sample 3	703	0.299
low surface sample 2	672	0.280
low surface sample 1	661	0.277

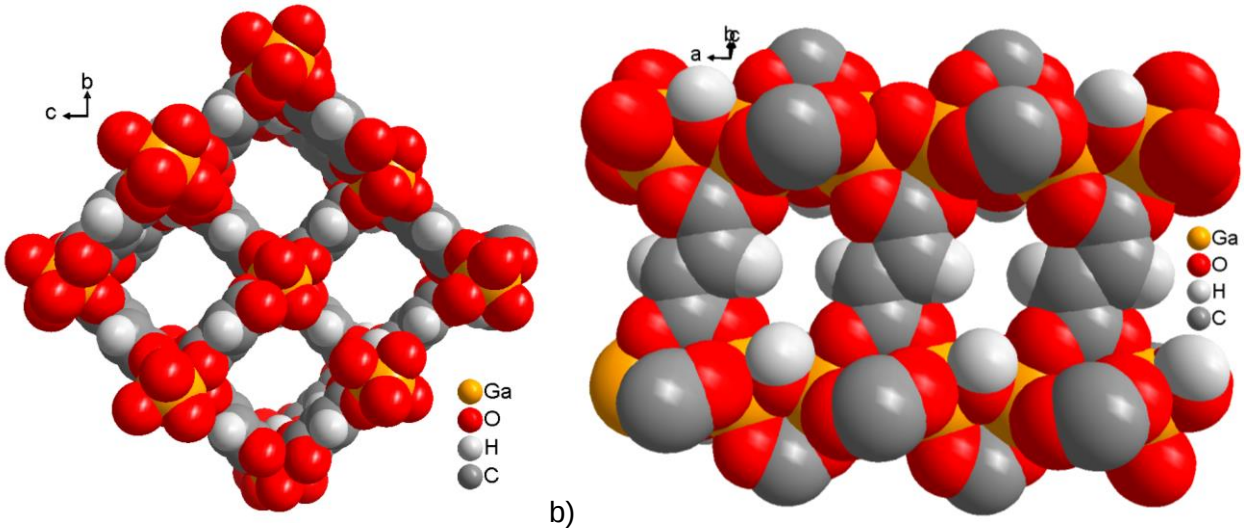

a) b)

Figure S7: a) Square channels along the a-axis and b) smaller channels perpendicular to *a* in Ga-fum. Redrawn from the deposited cif file with CCDC no. 1838533.[1]

Section S2: CO_2, CH_4 and H_2 gas sorption results and literature comparison

Table S2. Summary of the CO_2, CH_4 and H_2 gas uptakes at 1 bar and calculated zero coverage isosteric heat of adsorption values for HHUD-4 and In-fum.

	HHUD-4	In-fum
CO_2		
maximum uptake at 293 K [mmol g^{-1}]	2.74	1.76
maximum uptake at 273 K [mmol g^{-1}]	3.77	2.91
Q_{st}^0 [kJ mol^{-1}]	28.7	17.5
CH_4		
maximum uptake at 293 K [mmol g^{-1}]	0.72	0.56
maximum uptake at 273 K [mmol g^{-1}]	1.25	0.88
Q_{st}^0 [kJ mol^{-1}]	26.2	29.8
H_2		
maximum uptake at 100 K [mmol g^{-1}]	2.35	1.93
maximum uptake at 87 K [mmol g^{-1}]	4.34	3.45
maximum uptake at 77 K [mmol g^{-1}]	6.36	5.78
Q_{st}^0 [kJ mol^{-1}]	11.4	8.2

Table S3. Summary of the literature reported CO_2, CH_4 and H_2 uptakes at 1 bar and heat of adsorption values for various MOFs.

MOF	CO_2 uptake at 293 K [mmol g^{-1}]	CO_2 Q_{st}^0 [kJ mol^{-1}]	CH_4 uptake at 293 K [mmol g^{-1}]	CH_4 Q_{st}^0 [kJ mol^{-1}]	H_2 uptake at 77 K [mmol g^{-1}]	H_2 Q_{st}^0 [kJ mol^{-1}]
Zr-HHU-1	0.9[3]	60[3]	–	–	4.10[3]	10.3[3]
Ce-HHU-1	2.5[4]	47[4]	–	–	–	–
Hf-HHU-1	1.6[5]	39[5]	–	–	–	–
NUS-36	2.1[6,a]	–	–	–	–	–
MIL-53	2.11[7]	25[8]	0.57[9]	15[9,b]	1.47[13]	–
CAU-10-H	2.76[7]	25[10,b]	1.04[11]	8[9,b]	6.42[13]	–
Al-fum	2.52[7]	–	1.14[9]	15.9[9]	9.01[13]	–
MIL-160	4.22[7]	33[12]	0.84[11]	18.7[12]	11.91[13]	–
CAU-23	3.97[13]	22[13]	0.89[13]	14.8[13]	10.25[13]	4[13]
SNU-15’	–	–	–	–	3.66[14,c]	15.1[14]
Ni(dhtp)	–	–	–	–	–	12.9[15]
$Zn_3(bdc)_3[Cu(pyen)](DMF)_5(H_2O)_5$	–	–	–	–	–	12.3[16]

a: measured at 273 K, visually read from graph and calculated to mmol g^{-1} with the ideal gas equation $p \cdot v = n \cdot R \cdot T$

b: visually read from graph

c: calculated with ideal gas equation from uptake in cm^3 g^{-1}

Section S3: Calculations and fitting for the isosteric heat of adsorption of CO_2, CH_4 and H_2

Adsorption isotherms for CO_2, CH_4 (273 and 293 K) and H_2 (77, 87 and 100 K) of HHUD-4 and In-fum were fitted with the Freundlich-Langmuir model. Freundlich-Langmuir fits are given in Figure S8 to Figure S11 and the fitting parameters are summarized in Table S4 and Table S5.

Freundlich-Langmuir:

$$n = \frac{a \cdot b \cdot p^c}{1 + b \cdot p^c}$$

n = amount absorbed [mmol g^{-1}]

a = maximal loading [mmol g^{-1}]

b = affinity constant [bar^{-1}]

c = heterogeneity exponent

p = pressure [bar]

The isosteric heat of adsorption was then calculated with the Clausius-Clapeyron equation:

$$Q_{st} = -R\left(\frac{T_2 \cdot T_1}{T_2 - T_1}\right) ln\frac{p_2}{p_1}$$

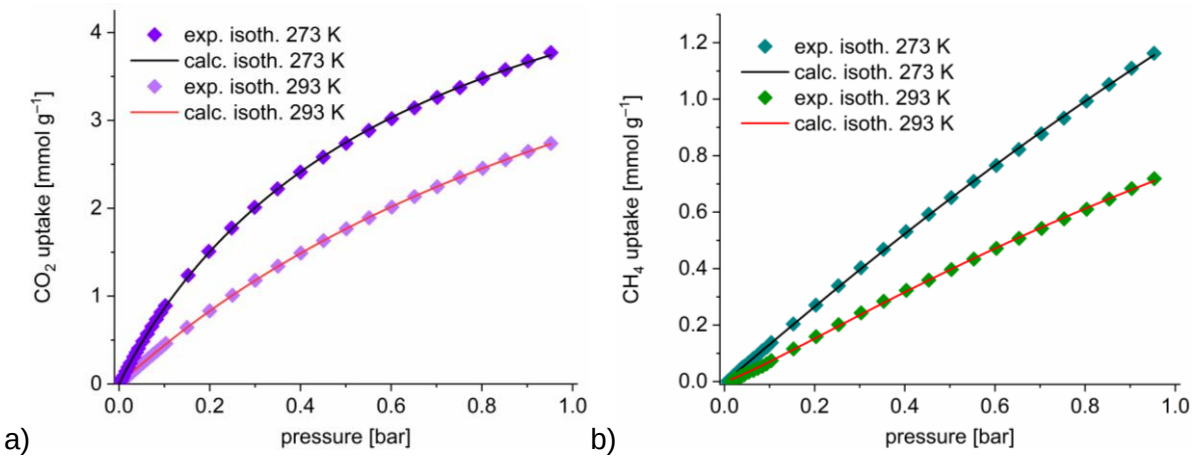

Figure S8. Experimental a) CO_2 and b) CH_4 adsorption isotherms of HHUD-4 with their corresponding Freundlich-Langmuir model fits at 273 and 293 K.

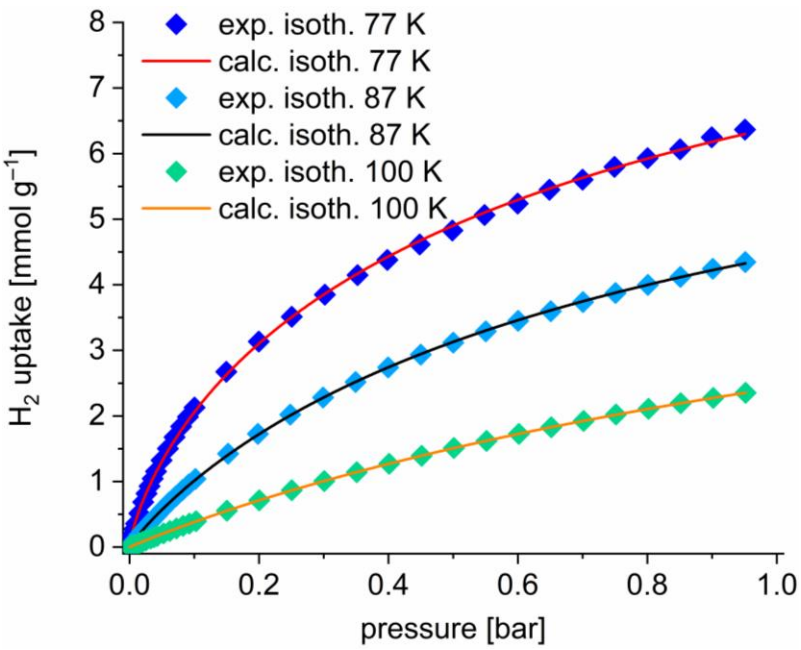

Figure S9. Experimental H_2 adsorption isotherms of HHUD-4 with their corresponding Freundlich-Langmuir model fits at 77, 87 and 100 K.

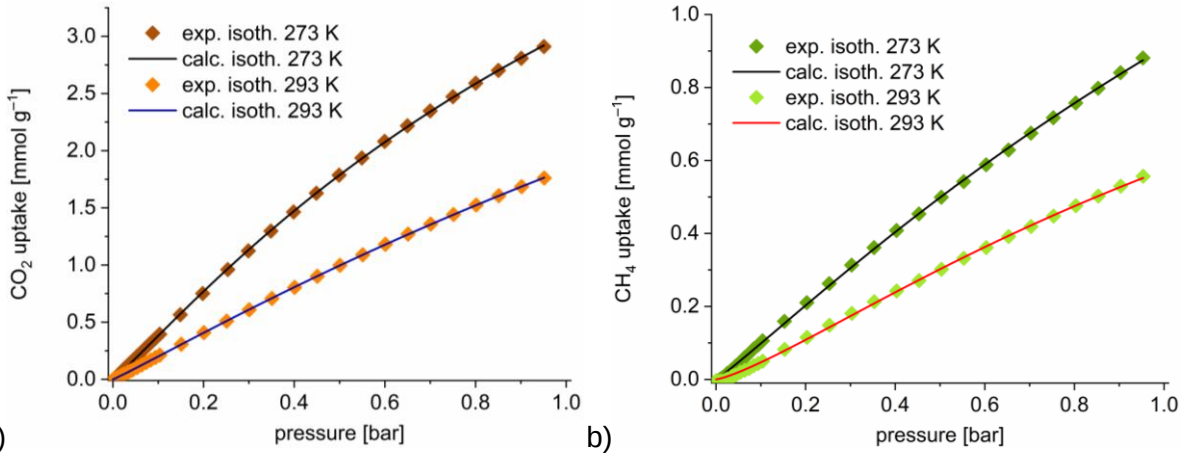

Figure S10. Experimental a) CO_2 and b) CH_4 adsorption isotherms of In-fum with their corresponding Freundlich-Langmuir model fits at 273 and 293 K.

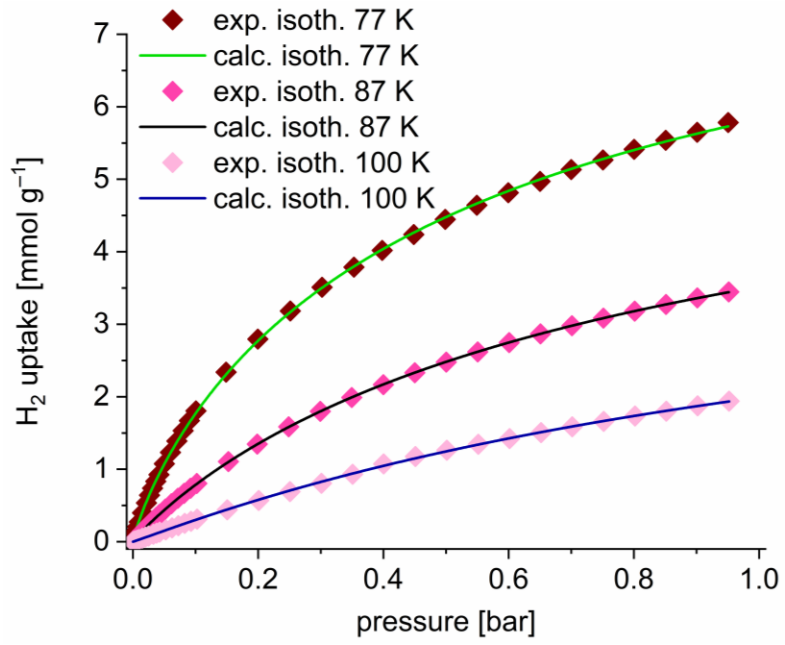

Figure S11. Experimental H_2 adsorption isotherms of In-fum with their corresponding Freundlich-Langmuir model fits at 77, 87 and 100 K.

Table S4. Freundlich-Langmuir fitting parameters for CO_2, CH_4 and H_2 adsorption isotherms for HHUD-4.

Gas	**CO_2**		**CH_4**		**H_2**		
Temperature [K]	273	293	273	293	77	87	100
maximal loading, *a* [mmol g^{-1}]*	6.3637	6.8862	6.5495	2.4905	11.4427	8.2774	6.5725
affinity constant, *b* [bar^{-1}]	1.4995	0.6913	0.2254	0.4223	1.2724	1.1462	0.5855
heterogeneity exponent, *c*	0.9803	1.0051	1.0418	1.1616	0.7639	0.9154	0.9766
Correlation coefficient R^2	0.99994	0.99998	0.99988	0.99973	0.99959	0.99994	0.99999
Heat of adsorption [kJ mol^{-1}]	28.7		26.2		11.4		

*amount adsorbed at saturation, that is maximal loading for the asymptotic curvature of the adsorption isotherm

Table S5. Freundlich-Langmuir fitting parameters for CO_2, CH_4 and H_2 adsorption isotherms for In-fum.

Gas	**CO_2**		**CH_4**		**H_2**		
Temperature [K]	273	293	273	293	77	87	100
maximal loading, *a* [mmol g^{-1}]*	7.7913	8.5030	3.4056	1.5839	9.2512	6.4966	4.6511
affinity constant, *b* [bar^{-1}]	0.6337	0.2760	0.3642	0.5684	1.6997	1.1804	0.7492
heterogeneity exponent, *c*	1.0906	1.0579	1.0873	1.2708	0.8568	0.9337	1.0345
Correlation coefficient R^2	0.99997	0.99998	0.99968	0.99919	0.99989	0.99999	0.99984
Heat of adsorption [kJ mol^{-1}]	17.5		29.8		8.2		

*amount adsorbed at saturation, that is maximal loading for the asymptotic curvature of the adsorption isotherm

Section S4: Fitting and IAST calculations for CO_2/CH_4 mixtures

The adsorption isotherms for CO_2 and CH_4 were fitted with the 3PSim software.[17] 3PSim is a tool to interpret and evaluate experimental adsorption data with several adsorption isotherm models, including Henry, Toth, Freundlich, LAI, SIPS, Dual-site Langmuir and DS Langmuir SIPS. The best fitting model for the CO_2 and CH_4 adsorption isotherms was the Toth model (a calculation of IAST with a Freundlich-Langmuir fit is not possible with the 3PSim software).

Toth:

$$q = q_{max} \frac{k \cdot p}{[1 + (k \cdot p)^t]^{\frac{1}{t}}}$$

q = amount absorbed [mmol g^{-1}]

q_{max} = maximal loading [mmol g^{-1}]

k = Toth constant/ affinity constant [bar^{-1}]

t = heterogeneity exponent

p = pressure [bar]

The IAST (ideal adsorbed solution theory) selectivity calculation was done with the "IAST with Toth" isotherm model with two components. The parameters (of both gases at a single temperature) obtained from the Toth fit (Table S6 and Table S7) were used as input, the molar fraction was set to 0.5 and the total pressure was set to 1 bar. From the resulting adsorbed fractions of CO_2 (x_1) and CH_4 (x_2) the selectivity was calculated with the following formula:

$$S = \frac{x_1/x_2}{y_1/y_2}$$

y_1 and y_2 are the mole fractions of CO_2 and CH_4, respectively.

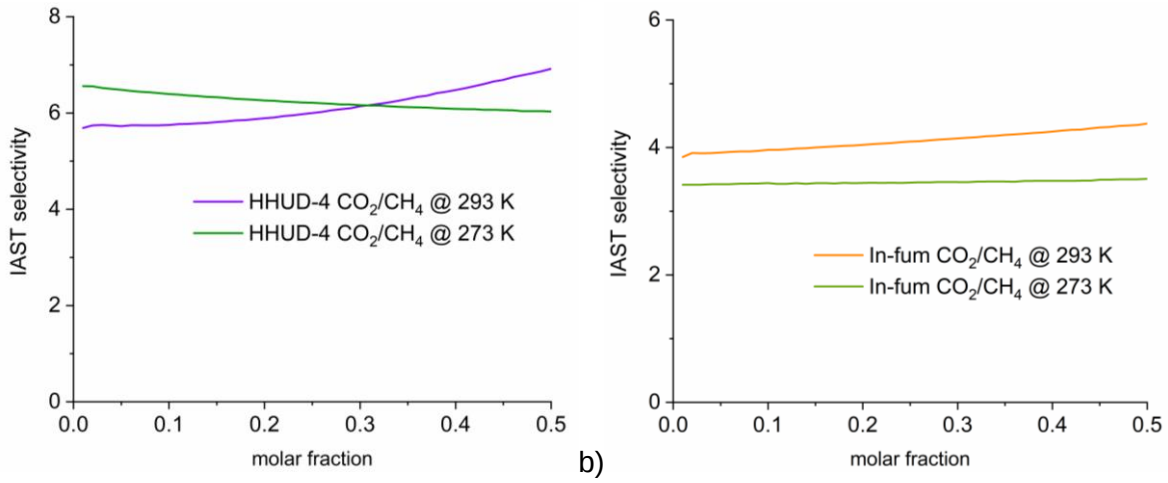

Figure S12. Plots of IAST selectivity of a) HHUD-4 and b) In-fum for CO_2/CH_4 mixtures at 273 and 293 K.

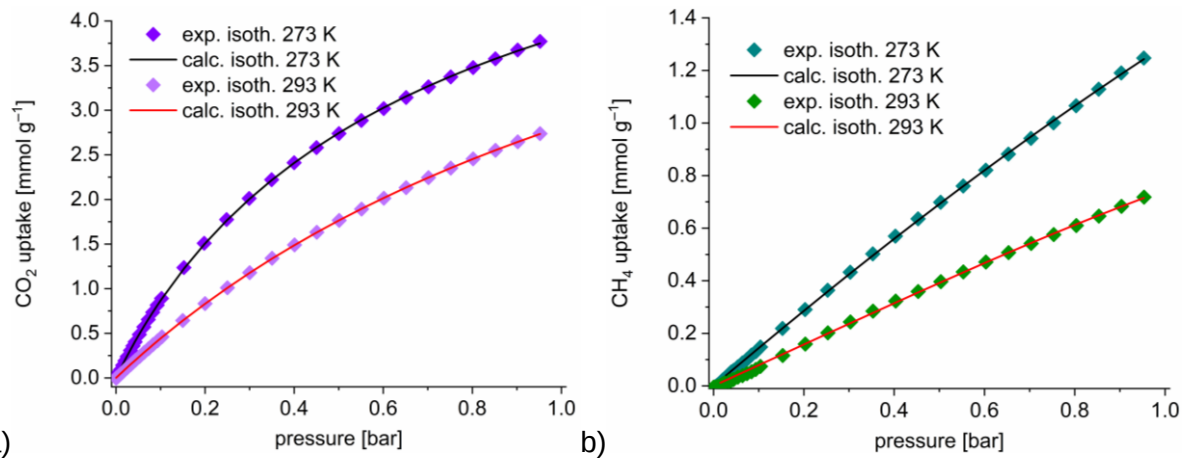

Figure S13. Experimental a) CO_2 and b) CH_4 adsorption isotherms of HHUD-4 with their corresponding Toth model fits at 273 and 293 K.

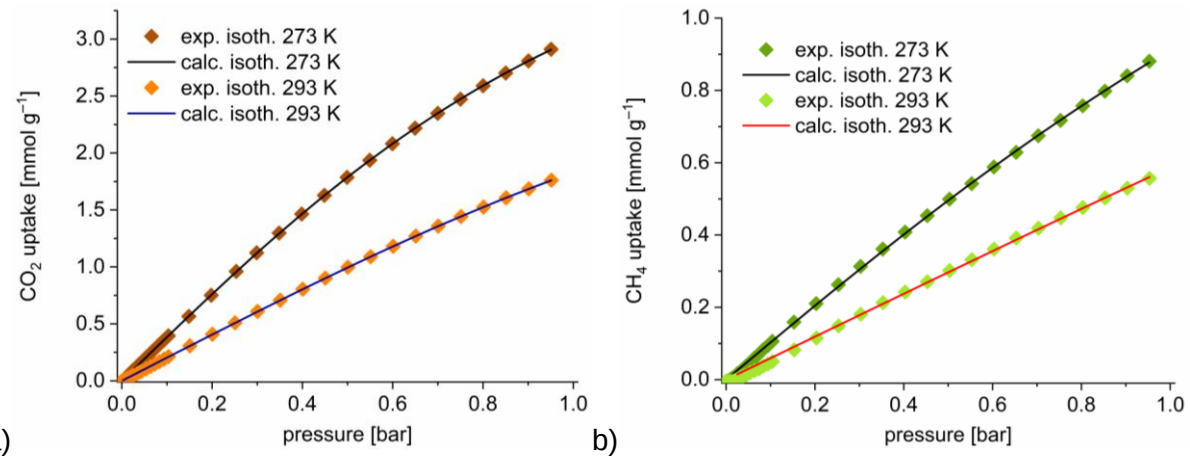

Figure S14. Experimental a) CO_2 and b) CH_4 adsorption isotherms of In-fum with their corresponding Toth model fits at 273 and 293 K.

Table S6. Toth fitting parameters for CO_2 and CH_4 adsorption isotherms for HHUD-4.

Gas	**CO_2**		**CH_4**	
Temperature [K]	273	293	273	293
maximal loading, q_{max} [mmol g^{-1}]*	6.731296	6.977597	5.499398	1.309495
affinity constant, k [bar^{-1}]	1.551246	0.675349	0.263016	0.602038
heterogeneity exponent, t	0.9086	1.0021	1.3643	3.1753
Correlation coefficient R^2	0.999954	0.999983	0.999834	0.999092

*amount adsorbed at saturation, that is maximal loading for the asymptotic curvature of the adsorption isotherm

Table S7. Toth fitting parameters for CO_2 and CH_4 adsorption isotherms for In-fum.

Gas	**CO_2**		**CH_4**	
Temperature [K]	273	293	273	293
maximal loading, q_{max} [mmol g^{-1}]*	4.722194	3.519293	2.388246	1.633522
affinity constant, k [bar^{-1}]	0.815456	0.578060	0.432077	0.363842
heterogeneity exponent, t	2.0282	2.3315	1.7211	3.1443
Correlation coefficient R^2	0.999987	0.999975	0.999630	0.997794

*amount adsorbed at saturation, that is maximal loading for the asymptotic curvature of the adsorption isotherm

Table S8. Calculated IAST-selectivities for CO_2 and CH_4 mixtures at 273 and 293 K for HHUD-4 and In-fum at selected molar fractions.

MOF	**Gases (X_1 and X_2) at T**	**IAST selectivity at molar fraction** (rounded to the next integer value)	
		0.01	**0.5**
HHUD-4	CO_2 and CH_4 at 273 K	7	6
	CO_2 and CH_4 at 293 K	6	7
In-Fum	CO_2 and CH_4 at 273 K	3	4
	CO_2 and CH_4 at 293 K	4	4

Section S5: Vapor sorption experiments

Table S9. Benzene, cyclohexane and n-hexane uptake for HHUD-4 and In-fum at specific p/p_0 values.

p/p_0	HHUD-4	In-fum
benzene uptake [mg g^{-1}] (% of maximum uptake)		
0.02	98 (36 %)	78 (28 %)
0.05	165 (61 %)	114 (41 %)
0.08	182 (68 %)	134 (48 %)
0.1	190 (71 %)	147 (53 %)
0.3	219 (81 %)	194 (70 %)
0.9	269	278
cyclohexane uptake [mg g^{-1}] (% of maximum uptake)		
0.02	41 (35 %)	34 (38 %)
0.05	82 (71 %)	40 (45 %)
0.08	87 (75 %)	43 (48 %)
0.1	89 (77 %)	46 (52 %)
0.3	98 (84 %)	57 (64 %)
0.9	116	89
n-hexane uptake [mg g^{-1}] (% of maximum uptake)		
0.02	71 (35 %)	150 (61 %)
0.05	118 (58 %)	160 (65 %)
0.08	126 (61 %)	165 (67 %)
0.1	129 (63 %)	169 (69 %)
0.3	149 (73 %)	189 (77 %)
0.9	205	245

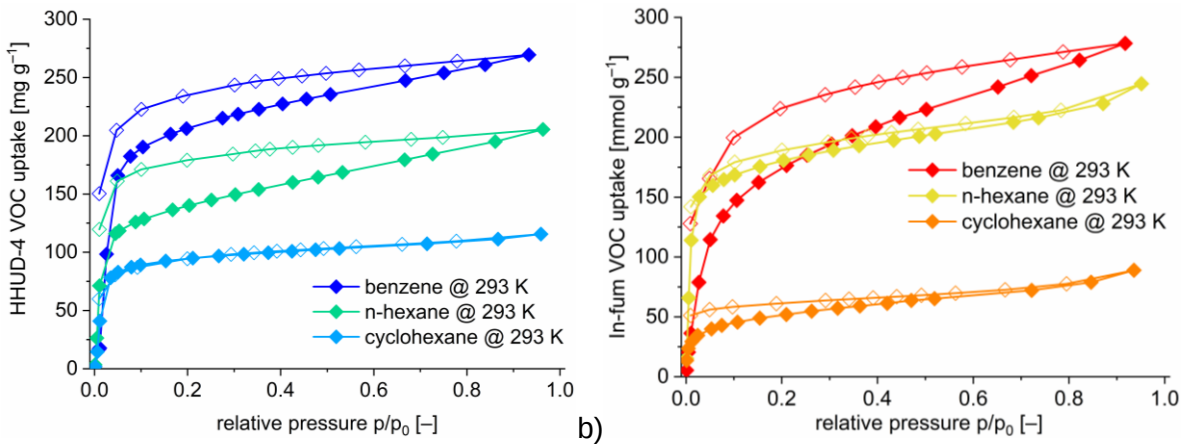

Figure S15. Benzene, cyclohexane and n-hexane vapor sorption isotherms at 293 K for a) HHUD-4 and b) In-fum [filled symbols for adsorption, empty symbols for desorption].

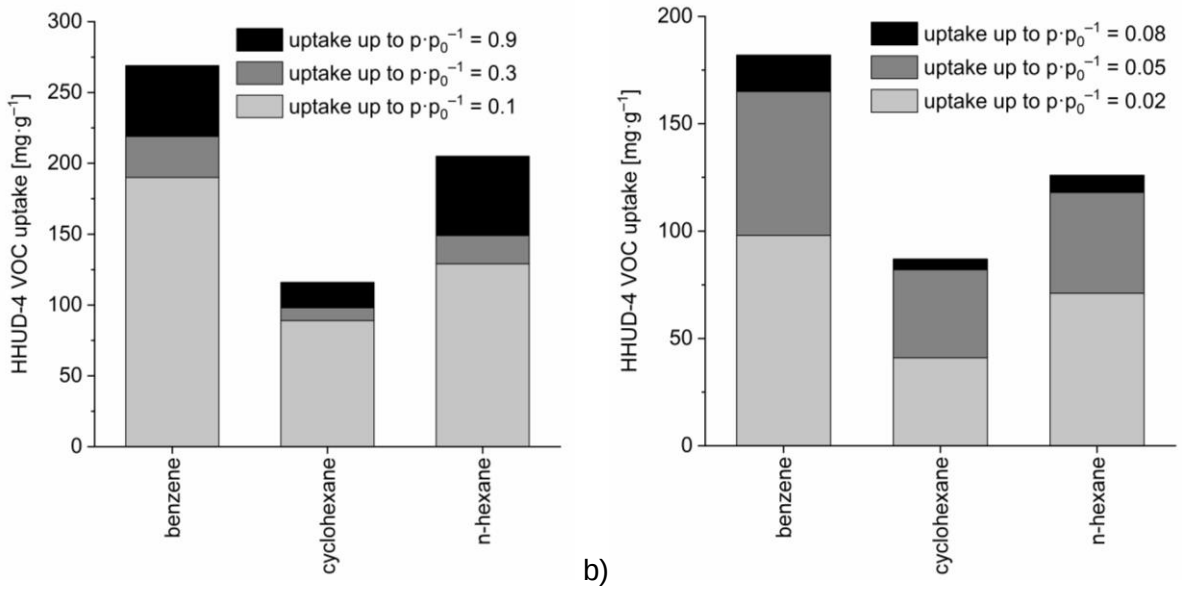

Figure S16. Benzene, cyclohexane and n-hexane uptake capacity at 293 K of HHUD-4 at different relative pressures a) p/p_0 = 0.1, 0.3 and 0.9 and b) p/p_0 = 0.02, 0.05 and 0.08 (specific values in Table S9).

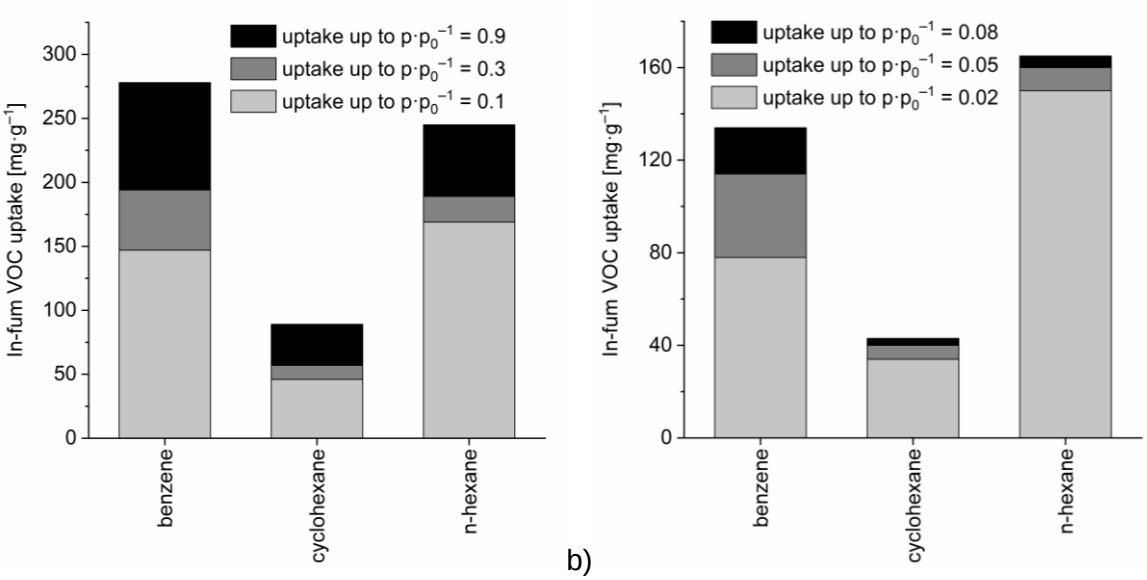

Figure S17. Benzene, cyclohexane and n-hexane uptake capacity at 293 K of In-fum at different relative pressures a) p/p_0 = 0.1, 0.3 and 0.9 and b) p/p_0 = 0.02, 0.05 and 0.08 (specific values in Table S9).

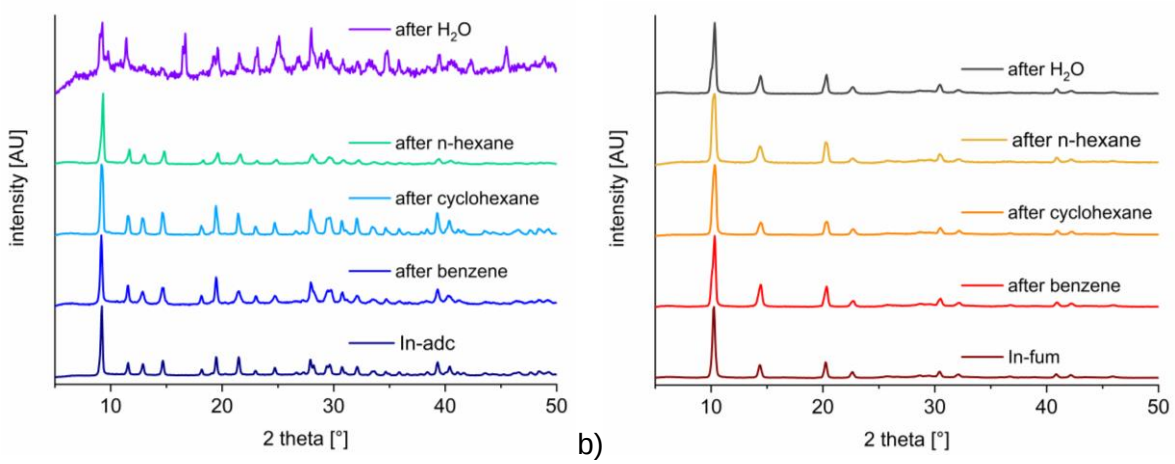

Figure S18. PXRD diffraction patterns of a) HHUD-4 and b) In-fum before and after vapor sorption experiments with benzene, cyclohexane, n-hexane and water.

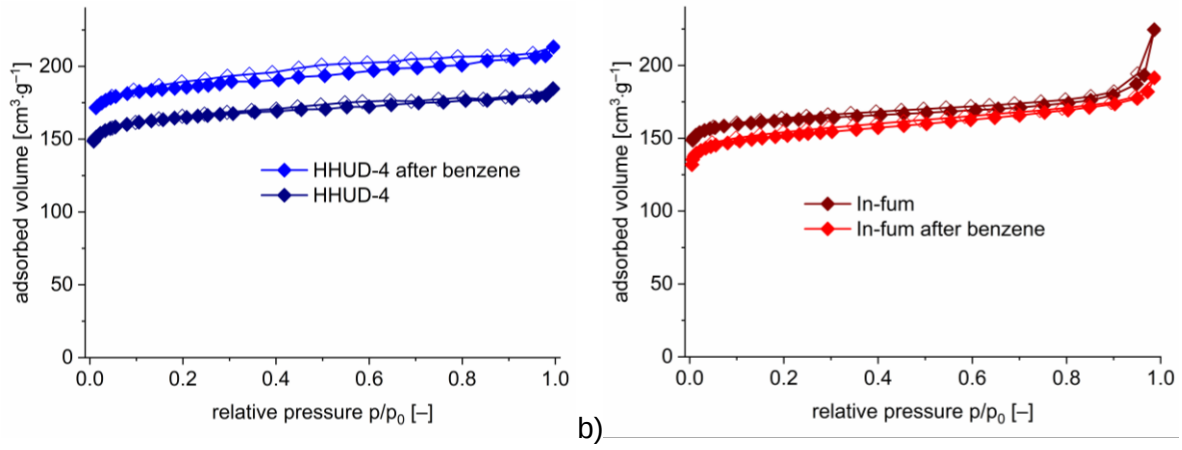

Figure S19. Volumetric nitrogen sorption measurements at 77 K of a) HHUD-4 and b) In-fum before and after benzene vapor sorption experiment (filled symbols for adsorption, empty symbols for desorption).

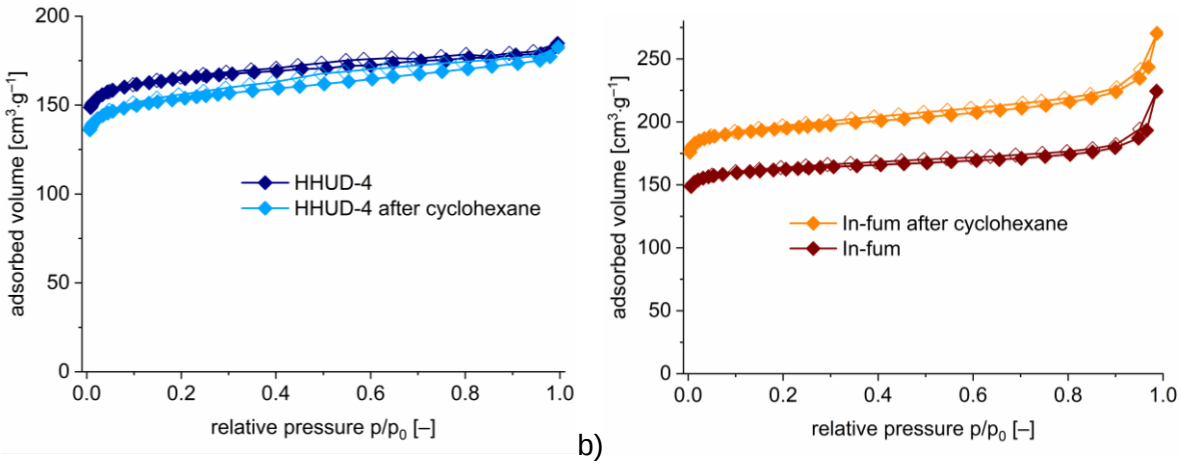

Figure S20. Volumetric nitrogen sorption measurements at 77 K of a) HHUD-4 and b) In-fum before and after cyclohexane vapor sorption experiment (filled symbols for adsorption, empty symbols for desorption).

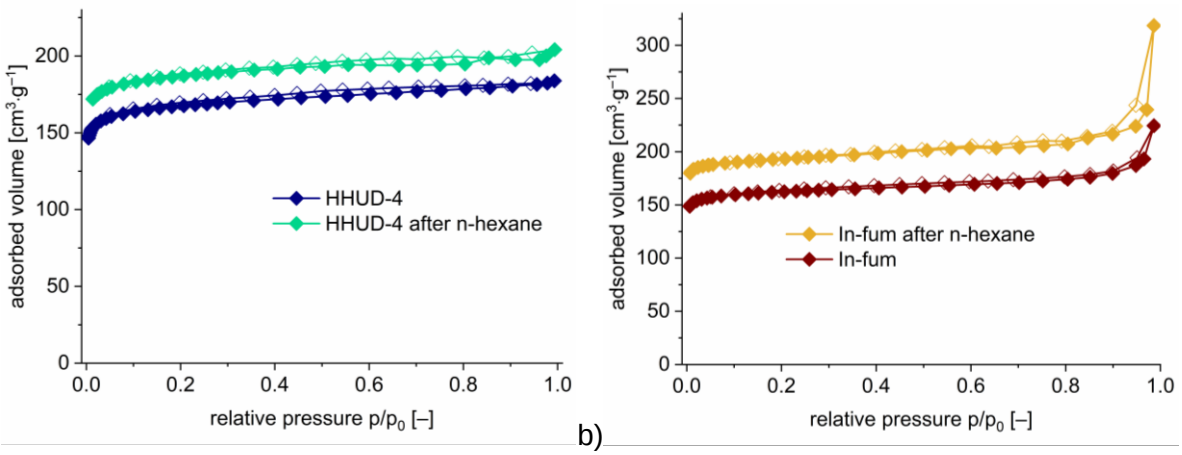

Figure S21. Volumetric nitrogen sorption measurements at 77 K of a) HHUD-4 and b) In-fum before and after n-hexane vapor sorption experiment (filled symbols for adsorption, empty symbols for desorption).

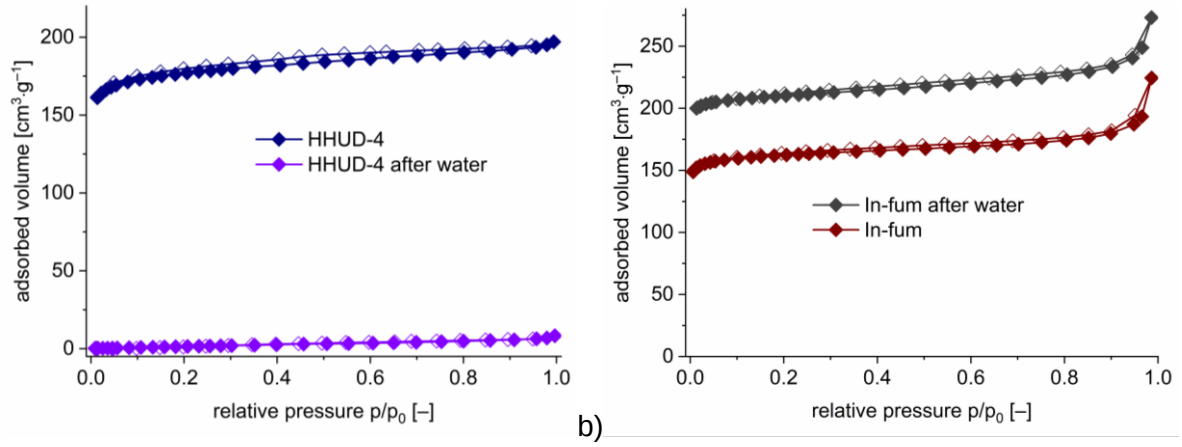

Figure S22. Volumetric nitrogen sorption measurements at 77 K of a) HHUD-4 and b) In-fum before and after water vapor sorption experiment (filled symbols for adsorption, empty symbols for desorption).

Table S10. BET surface areas and pore volume of HHUD-4 and In-fum samples after vapor sorption experiments.

sample	BET surface area [$m^2\ g^{-1}$]	pore volume at $p/p_0 = 0.95$ [$cm^3\ g^{-1}$]
HHUD-4 before VOC sorption	661	0.277
HHUD-4 after benzene	746	0.319
HHUD-4 after cyclohexane	613	0.271
HHUD-4 after n-hexane	745	0.305
HHUD-4 after water	~ 0	~ 0
In-fum before VOC sorption	661	0.289
In-fum after benzene	609	0.274
In-fum after cyclohexane	792	0.346
In-fum after n-hexane	791	0.346*
In-fum after water	867	0.371

*p/p_0 = 0.90, due to an increase in uptake (overlap with a type II isotherm at higher pressures)

Section S6: Fitting and IAST calculations for the vapor sorption experiments

Similar to the procedure in Section S4: Fitting and IAST calculations for CO_2/CH_4 mixtures, the adsorption isotherms for benzene, cyclohexane and n-hexane at 293 K were fitted with the 3PSim software.[17] For a better comparability all isotherms were fitted with the dual-site Langmuir Sips (DSLAISips) model. The pressure range above 0.09 bar for the cyclohexane adsorption isotherms of both HHUD-4 and In-fum were excluded from fitting to reduce the fitting error and obtain more accurate selectivities.

DSLAISips:

$$q_{eq} = q_{max}\left(\frac{K_1 \cdot p}{1 + K_1 \cdot p} + \frac{(K_2 \cdot p)^t}{(1 + K_2 \cdot p)^t}\right)$$

q_{eq}= amount adsorbed [mmol g^{-1}]

q_{max} = maximal loading [mmol g^{-1}]

K_1 and K_2 = affinity constant for adsorption [bar^{-1}]

p = pressure [bar]

t = heterogeneity exponent

The IAST (ideal adsorbed solution theory) selectivity calculation were done with the “IAST with DSLAISips” isotherm model with two components. The selectivities were calculated over a pressure range of the fitted isotherms from 0 to 0.09 bar with a constant vapor composition of 50:50 of both VOCs with the following formula:

$$S = \frac{x_1/x_2}{y_1/y_2}$$

where y_1 and y_2 are the molar fractions of the VOC and x_1 and x_2 are represents the adsorbed vapor amount.

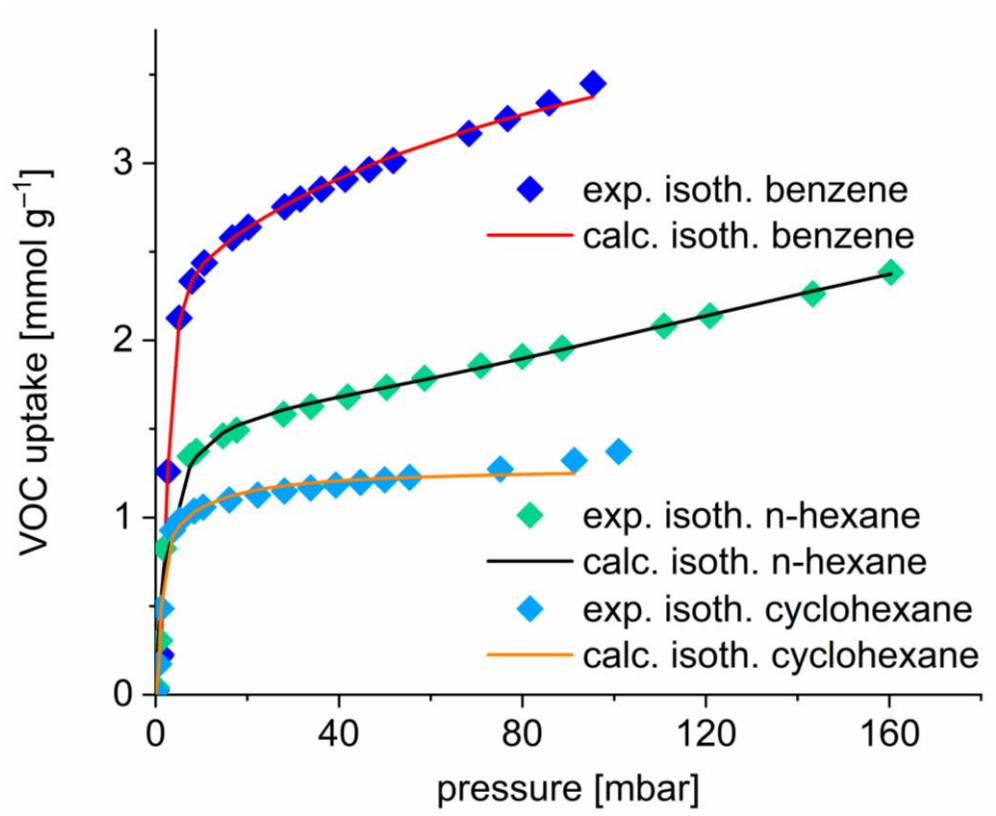

Figure S23. Experimental benzene, cyclohexane and n-hexane adsorption isotherms of HHUD-4 at 293 K with their corresponding DSLAISips model fits.

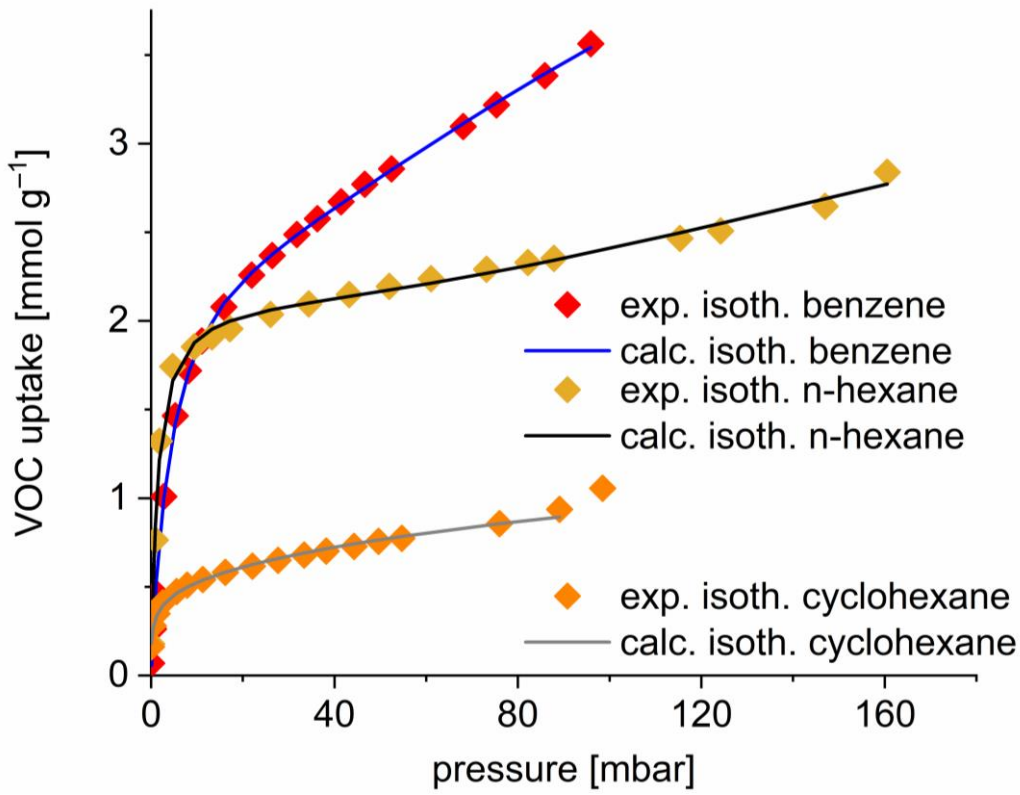

Figure S24. Experimental benzene, cyclohexane and n-hexane adsorption isotherms of In-fum at 293 K with their corresponding DSLAISips model fits.

Table S11. DSLAISips fitting parameters for benzene, cyclohexane and n-hexane adsorption isotherms for HHUD-4.

Vapor	benzene	cyclohexane	n-hexane
maximal loading, q_{max} [mmol g^{-1}]	2.255265	0.642721	1.724326
affinity constant, K_1 [bar^{-1}]	10.317593	180.740683	394.354743
affinity constant, K_2 [bar^{-1}]	396.315605	910.177530	5.066080
heterogeneity exponent, *t*	2.831478	3.891550	2.094568
Correlation coefficient R^2	0.999432	0.994705	0.992522

Table S12. DSLAISips fitting parameters for benzene, cyclohexane and n-hexane adsorption isotherms for In-fum.

Vapor	benzene	cyclohexane	n-hexane
maximal loading, q_{max} [mmol g^{-1}]	2.649726	0.829770	2.151630
affinity constant, K_1 [bar^{-1}]	217.494087	5.493819	722.691922
affinity constant, K_2 [bar^{-1}]	8.201325	252.500453	4.165343
heterogeneity exponent, *t*	1.995158	0.348853	2.142852
Correlation coefficient R^2	0.999661	0.994578	0.993071

Table S13. Calculated IAST-selectivities for different VOC-mixtures for HHUD-4 and In-fum at selected pressures.

MOF	VOC (X_1 and X_2)	IAST Selectivity for X_1/X_2 (rounded to the next integer value)		
		10 mbar	50 mbar	90 mbar
HHUD-4	benzene and cyclohexane	2	9	17
	benzene and *n*-hexane	1	3	3
	n-hexane and cyclohexane	2	3	3
In-Fum	benzene and cyclohexane	3	14	23
	benzene and *n*-hexane	2	2	1
	n-hexane and cyclohexane	13	37	46

Section S7: Theoretical calculations with the HHUD-4 crystal structure data

Table S14. Theoretical surface area and pore volume of HHUD-4.

Mercury 'void' calculation[2]	
Probe radius 1.2 Å, grid spacing 0.7 Å Void volume [Å^3] (% of unit cell) specific [cm^3 g^{-1}]	 773 (63) 0.48
Probe radius 0.7 Å, grid spacing 0.7 Å Void volume [Å^3] (% of unit cell) specific [cm^3 g^{-1}]	 790 (64) 0.49
Platon 'Calc Void'[18,19]	
Total potential solvent area [Å^3] (% of unit cell) specific [cm^3 g^{-1}]	738 (60) 0.46
CrystalExplorer 'Crystal voids' calculation[20,21]	
Surface area $S_{unit\ cell}$ (isovalue 0.002) [Å^2] specific [m^2 g^{-1}]	362 2235
Surface area $S_{unit\ cell}$ (isovalue 0.003) [Å^2] specific [m^2 g^{-1}]	364 2247
Pore volume (isovalue 0.002) [Å^3] specific [cm^3 g^{-1}]	716 0.44
Pore volume (isovalue 0.003) [Å^3] specific [cm^3 g^{-1}]	761 0.47

Theoretical specific surface areas are calculated according to $(S_{Unit\ Cell} \cdot N_A)/(Z \cdot M)$ and theoretical specific pore volumes are calculated according to $(\text{Void Volume} \cdot N_A)/(Z \cdot M)$ or $(\text{Solvent Accessible Volume} \cdot N_A)/(Z \cdot M)$;

Z = 4 (number of asymmetric formula units), N_A = Avogadro's constant: $6.022 \cdot 10^{23}$ mol^{-1}, M = 243.87 g mol^{-1} (molecular weight of the asymmetric formula unit).

Topology analysis for HHUD-4 with ToposPro and the Topcryst database[22,23,24,25]

```
#########################################################
1:C4 H In O5 + solvent/intercluster bonds for rings>6
#########################################################

Topology for Bk1
--------------------
Atom Bk1 links by bridge ligands and has
Common vertex with                    R(A-A)
Bk 1    1.5000    0.5000    0.3750   ( 1 0 0)    9.802A      1
Bk 1    0.5000   -0.5000    0.3750   ( 0-1 0)    9.802A      1
```

Bk 1 -0.5000 0.5000 0.3750 (-1 0 0) 9.802A 1

Bk 1 0.5000 1.5000 0.3750 (0 1 0) 9.802A 1

Structural group analysis

Structural group No 1

Structure consists of plane layers (0 0 1) with Bk

Num. groups=4; Thickness=4.00; Distances to Neighbors=3.203; 3.203

Coordination sequences

Bk1: 1 2 3 4 5 6 7 8 9 10

Num 4 8 12 16 20 24 28 32 36 40

Cum 5 13 25 41 61 85 113 145 181 221

TD10=221

Vertex symbols for selected sublattice

Bk1 Point symbol:{4^4.6^2}

Extended point symbol:[4.4.4.4.6(2).6(2)]

Point symbol for net: {4^4.6^2}

4-c net; uninodal net

You have to increase Max.Ring value to compute plane net VS correctly!

Topological type: **sql** (topos&RCSR.ttd) {4^4.6^2} - VS [4.4.4.4.*.*] (17828 types in 4 databases)

Elapsed time: 3.80 sec.

Section S8: HHUD-4 crystal data

Refinement

The hydrogen atoms for OH were positioned geometrically (O—H = 0.98 Å) and refined using a riding model (AFIX 148) with U_{iso}(H) = 1.5U_{eq}.

Computing details

Data collection: *APEX2* (Bruker, 2012); cell refinement: *SAINT* (Bruker, 2012); data reduction: *SAINT* (Bruker, 2012); program(s) used to solve structure: SHELXT-2015 (Sheldrick 2015a); program(s) used to refine structure: *SHELXL2017*/1 (Sheldrick, 2015b); molecular graphics: *DIAMOND* 4.3.1 (Brandenburg, 1999); software used to prepare material for publication: *SHELXL2017*/1 (Sheldrick, 2015b).

References

Bruker AXS. (2012). *APEX2*, *SAINT*. Bruker AXS Inc., Madison, Wisconsin, USA. Brandenburg, K. (1999). *DIAMOND*. Crystal Impact GbR, Bonn, Germany. Sheldrick, G. M. (1996). *SADABS*. University of Göttingen, Germany. Sheldrick, G. M. (2008). Acta Cryst. A64, 112-122. Sheldrick, G. M. (2015a). Acta Cryst. A71, 3-8. Sheldrick, G. M. (2015b). Acta Cryst. C71, 3-8.

S8.1 Crystal 1 *(In-adc_P4₁22)*

Crystal data

$C_4HInO_5^+$solvent	D_x = 1.316 Mg m^{-3}
M_r = 243.87	Mo $K\alpha$ radiation, λ = 0.71073 Å
Tetragonal, $P4_122$	Cell parameters from 6739 reflections
a = 9.8021 (7) Å	θ = 2.6–26.4°
c = 12.812 (1) Å	μ = 1.90 mm^{-1}
V = 1231.0 (2) Å^3	T = 140 K
Z = 4	Octahedral, clear colourless
F(000) = 456	0.31 × 0.18 × 0.17 mm

Data collection

Bruker Kappa APEX-II CCD area detector diffractometer	1284 independent reflections
Radiation source: microfocus sealed tube	1266 reflections with $I > 2\sigma(I)$
Multilayer mirror monochromator	R_{int} = 0.023
ω scans, ϕ scans	θ_{max} = 26.5°, θ_{min} = 2.1°
Absorption correction: multi-scan (*SADABS*; Sheldrick, 1996)	h = -12→11
T_{min} = 0.882, T_{max} = 1.000	k = -12→12
8314 measured reflections	l = -16→12

Refinement

Refinement on F^2	Secondary atom site location: difference Fourier map
Least-squares matrix: full	Hydrogen site location: inferred from neighbouring sites
$R[F^2 > 2\sigma(F^2)] = 0.009$	H-atom parameters constrained
$wR(F^2) = 0.025$	$w = 1/[\sigma^2(F_o^2) + (0.0096P)^2 + 0.2009P]$ where $P = (F_o^2 + 2F_c^2)/3$
$S = 1.13$	$(\Delta/\sigma)_{max} = 0.001$
1284 reflections	$\Delta\rangle_{max} = 0.21$ e Å^{-3}
47 parameters	$\Delta\rangle_{min} = -0.30$ e Å^{-3}
0 restraints	Absolute structure: Flack x determined using 476 quotients [(I+)-(I-)]/[(I+)+(I-)] (Parsons, Flack and Wagner, Acta Cryst. B69 (2013) 249-259).
Primary atom site location: structure-invariant direct methods	Absolute structure parameter: -0.017 (17)

Fractional atomic coordinates and isotropic or equivalent isotropic displacement parameters (Å^2) for crystal 1 (In-adc_P4$_1$22)

	x	*y*	*z*	U_{iso}*/U_{eq}
In1	0.500000	0.61899 (2)	0.500000	0.01067 (6)
O1	0.48535 (15)	0.48535 (15)	0.375000	0.0160 (4)
H1	0.416816	0.416815	0.375001	0.019*
C1	0.5564 (2)	0.8056 (2)	0.31063 (15)	0.0187 (4)
O2	0.48882 (19)	0.78840 (13)	0.39190 (10)	0.0226 (3)
C2	0.5553 (2)	0.9440 (2)	0.26710 (16)	0.0241 (4)
O3	0.62843 (14)	0.72099 (12)	0.26194 (10)	0.0202 (3)

Atomic displacement parameters (Å^2) for crystal 1 (In-adc_P4$_1$22)

	U^{11}	U^{22}	U^{33}	U^{12}	U^{13}	U^{23}
In1	0.01167 (9)	0.01214 (9)	0.00819 (8)	0.000	0.00052 (7)	0.000
O1	0.0184 (6)	0.0184 (6)	0.0114 (7)	-0.0076 (10)	0.0037 (5)	-0.0037 (5)
C1	0.0247 (10)	0.0153 (9)	0.0162 (9)	-0.0003 (8)	-0.0028 (8)	0.0025 (8)
O2	0.0327 (8)	0.0173 (6)	0.0180 (6)	0.0045 (7)	0.0035 (7)	0.0043 (5)
C2	0.0363 (11)	0.0173 (8)	0.0186 (10)	0.0004 (8)	0.0040 (9)	0.0010 (8)
O3	0.0275 (7)	0.0122 (6)	0.0208 (6)	-0.0030 (5)	0.0026 (7)	0.0002 (6)

Geometric parameters (Å, º) for crystal 1 (In-adc_P4$_1$22)

In1—O1	2.0740 (10)	O1—H1	0.9500
In1—O1^{i}	2.0740 (10)	C1—O2	1.245 (2)
In1—O2	2.1651 (12)	C1—O3	1.256 (2)
In1—O2^{ii}	2.1651 (12)	C1—C2	1.466 (3)
In1—O3^{iii}	2.1735 (12)	C2—C2^{iv}	1.183 (4)

In1—O3^{i}	2.1735 (12)		
O1—In1—O1^{i}	101.66 (6)	O2—In1—O3^{i}	87.82 (6)
O1—In1—O2	89.25 (5)	O2^{ii}—In1—O3^{i}	88.44 (6)
O1^{i}—In1—O2	169.08 (4)	O3^{iii}—In1—O3^{i}	175.12 (7)
O1—In1—O2^{ii}	169.08 (4)	In1^{v}—O1—In1	120.58 (10)
O1^{i}—In1—O2^{ii}	89.25 (5)	In1^{v}—O1—H1	119.7
O2—In1—O2^{ii}	79.84 (7)	In1—O1—H1	119.7
O1—In1—O3^{iii}	92.38 (5)	O2—C1—O3	128.67 (18)
O1^{i}—In1—O3^{iii}	90.70 (5)	O2—C1—C2	116.09 (18)
O2—In1—O3^{iii}	88.44 (6)	O3—C1—C2	115.21 (17)
O2^{ii}—In1—O3^{iii}	87.82 (6)	C1—O2—In1	127.73 (13)
O1—In1—O3^{i}	90.70 (5)	C2^{iv}—C2—C1	179.3 (3)
O1^{i}—In1—O3^{i}	92.38 (5)	C1—O3—In1^{v}	132.03 (13)

Symmetry codes: (i) -*y*+1, *x*, *z*+1/4; (ii) -*x*+1, *y*, -*z*+1; (iii) *y*, *x*, -*z*+3/4; (iv) *x*, -*y*+2, -*z*+1/2; (v) *y*, -*x*+1, *z*-1/4.

S8.2 Crystal 2 *(In-adc_P4$_3$22)*

Crystal data

C_4HInO_5	D_x = 1.318 Mg m^{-3}
M_r = 243.87	Mo $K\alpha$ radiation, λ = 0.71073 Å
Tetragonal, $P4_322$	Cell parameters from 6150 reflections
a = 9.8015 (9) Å	θ = 2.6–30.6°
c = 12.7970 (14) Å	μ = 1.90 mm^{-1}
V = 1229.4 (3) Å^3	T = 140 K
Z = 4	Octahedral, clear colourless
F(000) = 456	0.24 × 0.22 × 0.20 mm

Data collection

Bruker Kappa APEX-II CCD area detector diffractometer	1889 independent reflections
Radiation source: microfocus sealed tube	1843 reflections with $I > 2\sigma(I)$
Multilayer mirror monochromator	R_{int} = 0.018
ω scans, ϕ scans	θ_{max} = 30.6°, θ_{min} = 2.1°
Absorption correction: multi-scan (*SADABS*; Sheldrick, 1996)	h = -1111
T_{min} = 0.578, T_{max} = 0.685	k = -1114
7274 measured reflections	l = -1718

Refinement

Refinement on F^2	Hydrogen site location: inferred from neighbouring sites
Least-squares matrix: full	H-atom parameters constrained
$R[F^2 > 2\sigma(F^2)] = 0.013$	$w = 1/[\sigma^2(F_o^2) + (0.0169P)^2 + 0.2125P]$ where $P = (F_o^2 + 2F_c^2)/3$
$wR(F^2) = 0.034$	$(\Delta/\sigma)_{max} < 0.001$
$S = 1.08$	$\Delta\rangle_{max} = 0.90$ e Å^{-3}
1889 reflections	$\Delta\rangle_{min} = -0.24$ e Å^{-3}
47 parameters	Absolute structure: Flack x determined using 718 quotients [(I+)-(I-)]/[(I+)+(I-)] (Parsons, Flack and Wagner, Acta Cryst. B69 (2013) 249-259).
0 restraints	Absolute structure parameter: -0.009 (15)

Fractional atomic coordinates and isotropic or equivalent isotropic displacement parameters (Å²) for crystal 2 (In-adc_P4₃22)

	x	*y*	*z*	U_{iso}*/U_{eq}
In1	0.500000	0.38083 (2)	0.500000	0.01173 (5)
O1	0.48519 (14)	0.51481 (14)	0.375000	0.0171 (4)
H1	0.416656	0.583345	0.375000	0.020*
C1	0.5569 (2)	0.1942 (2)	0.31003 (14)	0.0197 (4)
O3	0.62898 (14)	0.27889 (13)	0.26160 (10)	0.0211 (3)
O2	0.48841 (19)	0.21166 (13)	0.39147 (10)	0.0238 (3)
C2	0.5559 (2)	0.0557 (2)	0.26727 (14)	0.0247 (4)

Atomic displacement parameters (Å²) for crystal 2 (In-adc_P4₃22)

	U^{11}	U^{22}	U^{33}	U^{12}	U^{13}	U^{23}
In1	0.01293 (8)	0.01347 (8)	0.00880 (7)	0.000	0.00052 (6)	0.000
O1	0.0196 (6)	0.0196 (6)	0.0121 (6)	0.0071 (8)	0.0034 (5)	0.0034 (5)
C1	0.0259 (10)	0.0160 (9)	0.0173 (8)	0.0009 (7)	-0.0042 (7)	-0.0017 (6)
O3	0.0277 (7)	0.0138 (6)	0.0217 (6)	0.0026 (5)	0.0023 (6)	-0.0003 (5)
O2	0.0330 (8)	0.0182 (6)	0.0202 (6)	-0.0050 (6)	0.0045 (6)	-0.0053 (5)
C2	0.0381 (12)	0.0173 (9)	0.0187 (9)	-0.0005 (7)	0.0023 (7)	-0.0016 (7)

Geometric parameters (Å, º) for crystal 2 (In-adc_P4₃22)

In1—O1^{i}	2.0747 (10)	O1—H1	0.9500
In1—O1	2.0747 (10)	C1—O2	1.252 (2)
In1—O2	2.1659 (13)	C1—O3	1.254 (2)
In1—O2^{ii}	2.1660 (13)	C1—C2	1.464 (3)
In1—O3^{i}	2.1745 (13)	C2—C2^{iv}	1.178 (4)
In1—O3^{iii}	2.1745 (13)		

O1^{i}—In1—O1	101.46 (6)	O2—In1—O3^{iii}	88.55 (6)
O1^{i}—In1—O2	169.31 (4)	O2^{ii}—In1—O3^{iii}	87.57 (6)
O1—In1—O2	89.23 (5)	O3^{i}—In1—O3^{iii}	174.93 (7)
O1^{i}—In1—O2^{ii}	89.23 (5)	In1^{v}—O1—In1	120.39 (10)
O1—In1—O2^{ii}	169.31 (4)	In1^{v}—O1—H1	119.8
O2—In1—O2^{ii}	80.09 (7)	In1—O1—H1	119.8
O1^{i}—In1—O3^{i}	92.58 (5)	O2—C1—O3	128.58 (18)
O1—In1—O3^{i}	90.62 (5)	O2—C1—C2	115.73 (18)
O2—In1—O3^{i}	87.57 (6)	O3—C1—C2	115.67 (17)
O2^{ii}—In1—O3^{i}	88.55 (6)	C1—O3—In1^{v}	131.96 (13)
O1^{i}—In1—O3^{iii}	90.62 (5)	C1—O2—In1	127.61 (13)
O1—In1—O3^{iii}	92.58 (5)	C2^{iv}—C2—C1	179.58 (15)

Symmetry codes: (i) *y*, -*x*+1, *z*+1/4; (ii) -*x*+1, *y*, -*z*+1; (iii) -*y*+1, -*x*+1, -*z*+3/4; (iv) *x*, -*y*, -*z*+1/2; (v) -*y*+1, *x*, *z*-1/4.

Section S9: References

1 Y. Zhang, B. E. G. Lucier, S. M. McKenzie, M. Arhangelskis, A. J. Morris, T. Friščić, J. W. Reid, V. V. Terskikh, M. Chen and Y. Huang, *ACS Appl Mater. Interfaces,* 2018, **10**, 28582.

2 C. F. Macrae, I. Sovago, S. J. Cottrell, P. T. A. Galek, P. McCabe, E. Pidcock, M. Platings, G. P. Shields, J. S. Stevens, M. Towler and P. A. Wood, *J. Appl. Crystallogr.,* 2020, **53**, 226.

3 T. J. Matemb Ma Ntep, H. Reinsch, B. Moll, E. Hastürk, S. Gökpinar, H. Breitzke, C. Schlüsener, L. Schmolke, G. Buntkowsky and C. Janiak, *Chemistry,* 2018, **24**, 14048.

4 T. J. Matemb Ma Ntep, H. Reinsch, J. Liang and C. Janiak, *Dalton Trans.,* 2019, **48**, 15849.

5 T. J. Matemb Ma Ntep, H. Reinsch, C. Schlüsener, A. Goldman, H. Breitzke, B. Moll, L. Schmolke, G. Buntkowsky and C. Janiak, *Inorg. Chem.,* 2019, **58**, 10965.

6 Y. Wang, S. Yuan, Z. Hu, T. Kundu, J. Zhang, S. B. Peh, Y. Cheng, J. Dong, D. Yuan, H.-C. Zhou and D. Zhao, *ACS Sustainable Chem. Eng.,* 2019, **7**, 7118.

7 P. Brandt, S.-H. Xing, J. Liang, G. Kurt, A. Nuhnen, O. Weingart, C. Janiak, *ACS Appl Mater Interfaces* 2021, **13**, 29137–29149.

8 B. C. Camacho, R. P. Ribeiro, I. A. Esteves and J. P. Mota, *Sep. Purif. Technol.,* 2015, **141**, 150.

9 Z. Huang, P. Hu, J. Liu, F. Shen, Y. Zhang, K. Chai, Y. Ying, C. Kang, Z. Zhang and H. Ji, *Sep. Purif. Technol.,* 2022, **286**, 120446.

10 J. Pei, H.-M. Wen, X.-W. Gu, Q.-L. Qian, Y. Yang, Y. Cui, B. Li, B. Chen and G. Qian, *Angew. Chem. Int. Ed.,* 2021, **60**, 25068.

11 D. Shade, B. Marszalek and K. S. Walton, *Adsorption,* 2021, **27**, 227.

12 D. Damasceno Borges, P. Normand, A. Permiakova, R. Babarao, N. Heymans, D. S. Galvao, C. Serre, G. de Weireld and G. Maurin, *J. Phys. Chem. C,* 2017, **121**, 26822.

13 C. Jansen, N. Tannert, D. Lenzen, M. Bengsch, S. Millan, A. Goldman, D. N. Jordan, L. Sondermann, N. Stock and C. Janiak, *Z. Anorg. Allg. Chem.,* 2022, **648**, e202200170.

14 Y. E. Cheon and M. P. Suh, *Chem. Commun.,* 2009, 2296.

15 W. Zhou, H. Wu and T. Yildirim, *J. Am. Chem. Soc.,* 2008, **130**, 15268.

16 B. Chen, X. Zhao, A. Putkham, K. Hong, E. B. Lobkovsky, E. J. Hurtado, A. J. Fletcher and K. M. Thomas, *J. Am. Chem. Soc.,* 2008, **130**, 6411.

17 3P INSTRUMENTS, 3P sim, Version 1.1.0.7, Simulation and Evaluation Tool for mixSorb, 3P INSTRUMENTS 2018.

18 Spek, A.L. PLATON – A Multipurpose Crystallographic Tool (Utrecht University, Utrecht, The Netherlands) 2008; Farrugia, L.J. Windows implementation, Version 270519 (University of Glasgow, Scotland) 2019.

19 A. L. Spek, *Acta. Crystallogr. D Biol. Crystallogr.,* 2009, **65**, 148.

20 M. J. Turner, J. J. McKinnon, D. Jayatilaka and M. A. Spackman, *CrystEngComm,* 2011, **13**, 1804.

21 J. J. McKinnon, M. A. Spackman and A. S. Mitchell, *Acta Crystallogr. B,* 2004, **60**, 627.

22 E. V. Alexandrov, A. P. Shevchenko and V. A. Blatov, *Cryst. Growth Des.,* 2019, **19**, 2604.

23 V. A. Blatov and D. M. Proserpio, *Acta Crystallogr. A Found Crystallogr.,* 2009, **65**, 202.

24 V. A. Blatov, A. P. Shevchenko and D. M. Proserpio, *Cryst. Growth Des.,* 2014, **14**, 3576.

25 E. V. Alexandrov, V. A. Blatov, A. V. Kochetkov and D. M. Proserpio, *CrystEngComm,* 2011, **13**, 3947.